

# An extrapolative approach to integration over hypersurfaces in the level set framework

Catherine Kublik\* and Richard Tsai†

November 4, 2016

## Abstract

We provide a new approach for computing integrals over hypersurfaces in the level set framework. In particular, this new approach is able to compute high order approximations of line or surface integrals in the case where the curve or surface has singularities such as corners. The method is based on the discretization (via simple Riemann sums) of the usual line or surface integral formulation used in the level set framework. This integral formulation involves an approximate Dirac delta function supported on a tubular neighborhood around the interface and is an *approximation* of the line or surface integral one wishes to compute. The novelty of this work is the choice of kernels used to approximate the Dirac delta function. We prove that for smooth interfaces, if the kernel has enough vanishing moments (related to the dimension of the space), the analytical integral formulation coincides exactly with the integral one wishes to calculate. For curves with singularities, the formulation is not exact but we provide an analytical result relating the severity of the singularity (corner or cusp) with the width of the tubular neighborhood. We show numerical examples demonstrating the capability of the approach, especially for integrating over piecewise smooth interfaces and for computing integrals where the integrand has an integrable singularity.

## 1 Introduction

This paper provides a new understanding of surface integrals in the level set framework particularly in the case where the curves or surfaces have singularities, for example corners for curves, and corners and edges for surfaces. It is of interest to study the integration over implicitly defined interfaces with singularities because there are many applications where surfaces have singularities in the context of level set methods. In the classical setting of level set techniques, it is very common for interfaces to develop singularities as they experience topological changes. In computer vision for example, a segmentation of an image can be obtained via a two dimensional flow using level set methods, in which case the flow will give rise to a curve undergoing topological changes and developing corners during its evolution. Level set methods have also been used in constrained optimization problems [9, 11], where the

---

\*Department of Mathematics, University of Dayton, 300 College Park, Dayton, OH 45469, USA . Email: ckublik1@udayton.edu.

†Department of Mathematics, KTH Royal Institute of Technology, SE-100 44, Stockholm, Sweden and Department of Mathematics and ICES, University of Texas at Austin, Austin, TX 78712, USA. Email: tsai@kth.se.

Lagrange multipliers can be expressed in terms of boundary integrals. In addition, boundary integral methods used in combination with level sets [6, 7, 1] have recently shown promising results. Other applications of implicit boundary integral methods include the computation of the Dirichlet-to-Neumann map in the context of shape optimization and the integration over streamlines in fluid mechanics. In this paper, we shed light on a mathematical framework for integrating over hypersurfaces with singularities defined implicitly via a level set function.

Let  $\Gamma_0$  be a closed hypersurface in  $\mathbb{R}^n$  (namely, a closed curve in  $\mathbb{R}^2$  or closed surface in  $\mathbb{R}^3$ ) defined implicitly as the zero level set of a level set function  $\phi$ , namely

$$\Gamma_0 := \{\mathbf{x} : \phi(\mathbf{x}) = 0\}. \quad (1)$$

We are interested in computing integrals of the form

$$I_0 := \int_{\Gamma_0} f(\mathbf{x}) dS(\mathbf{x}). \quad (2)$$

We focus on the situation where the information about  $\Gamma_0$  is given only via the values of  $\phi$  on some grid. We shall refer to the corresponding grid function by  $\phi_{\mathbf{i}}$ . There are two strategies for computing integrals like (2) in the level set framework:

1. (Type I) First discretize and then compute. From the level set grid function  $\phi_{\mathbf{i}}$  one can approximate the curve or surface  $\Gamma_0$  by  $\Gamma_{\Delta}$ , which is typically polygonal. The approximation  $\Gamma_{\Delta}$  is then used to compute the integral of  $f$  over  $\Gamma_0$  using local parameterizations of  $\Gamma_{\Delta}$  (see e.g. [8, 14, 17]).
2. (Type II) First derive an analytical integral formulation  $I(f, \phi)$  that is *easy* to discretize, then discretize it. We note that this approach computes the integral (2) *without using any local parameterizations of  $\Gamma_0$* .

In this paper, we consider the second approach. In the level set framework, the integral (2) is classically replaced by an integral of the form

$$\int_{\mathbb{R}^n} f(\mathbf{x}) \delta(\phi(\mathbf{x})) |\nabla \phi| d\mathbf{x},$$

where  $\delta(\cdot)$  typically denotes the Dirac delta function or in general a kernel that integrates to 1. The integral over  $\mathbb{R}^n$  is then discretized using simple Riemann sums and a specific choice for  $\delta(\cdot)$ . There are many approximations or regularizations of  $\delta(\cdot)$  in the numerical literature. Typically the regularized  $\delta$ -function is defined on a tubular neighborhood around the interface of width  $\epsilon$ , denoted  $\delta_{\epsilon}$ . One choice is to take  $\epsilon$  independent of the level set function  $\phi$  and the grid. In the work of Smereka [17], the discrete delta-function is concentrated within one grid cell on either side of the interface, and is obtained by discretizing the fundamental solution of the Laplace equation using ghost-points. In the work of Towers [18], the discretized delta function is computed via two different formulations involving the Heaviside function. The more accurate formulation is obtained using integration by parts on a suitable integral. In [5], the Dirac delta function is regularized using the gradient of the level set function  $\phi$ , a scaling that allows  $\epsilon$  (the width of the tubular neighborhood around the interface) to be small with respect to the underlying grid.

The framework for the present work started with [6] and [7] where the authors proposed and studied an integral formulation over the ambient space that coincides exactly with the

line or surface integral that one wishes to calculate. This formulation is designed for curves and surfaces that are not defined by any explicit parameterizations and is intended to be used with level set techniques [10, 12, 16]. In [7] the formulation is provided in dimensions two and three and extended to open curves and surfaces.

The integral formulation proposed in [6] and [7] allows the computation of integrals of the form (2), where  $\Gamma_0$  is the zero level set of the signed distance function  $d$  to  $\Gamma$ , namely  $\Gamma_0 := \{\mathbf{x} : d(\mathbf{x}) = 0\}$ . We remark that if one has a level set function  $\phi$  which is not the signed distance function to  $\Gamma_0$ , fast algorithms such as fast marching and fast sweeping [3, 13, 15, 19, 20] can be used to construct a signed distance function  $d$  to  $\Gamma_0$ . The integral formulation is given by

$$\int_{\mathbb{R}^n} f(P_{\Gamma_0}(\mathbf{x})) \delta_\epsilon(d(\mathbf{x})) J(\mathbf{x}; d(\mathbf{x})) d\mathbf{x}, \quad (3)$$

such that

$$\int_{\mathbb{R}^n} f(P_{\Gamma_0}(\mathbf{x})) \delta_\epsilon(d(\mathbf{x})) J(\mathbf{x}; d(\mathbf{x})) d\mathbf{x} = I_0, \quad (4)$$

where  $P_\Gamma : \mathbb{R}^n \mapsto \Gamma_0$  is the closest point mapping to  $\Gamma_0$  (or projection operator onto  $\Gamma_0$ ) defined as

$$P_{\Gamma_0}(\mathbf{x}) = \mathbf{x} - d(\mathbf{x}) \nabla d(\mathbf{x}), \quad (5)$$

$\delta_\epsilon$  is an averaging kernel satisfying some vanishing moment conditions and specifying a tubular neighborhood around  $\Gamma_0$ , and  $J(\mathbf{x}; d(\mathbf{x}))$  is the Jacobian that accounts for the change in curvature between nearby level sets and the zero level set  $\Gamma_0$ . The main advantage and novelty of formulation (3) is that unlike previous techniques in the level set framework (see later Equation (7)) which involve *approximating* the line or surface integral  $I_0$  using a regularized Dirac- $\delta$  function concentrated on  $\Gamma_0$  [4, 5, 17, 18, 21], (3) is equal to  $I_0$  analytically. Errors are therefore due only to the numerical scheme used to discretize (3) instead of both the numerical scheme and the anterior approximation.

For smooth curves or surfaces, the integral formulation (3) is very powerful: it provides a very elegant, simple and attractive computational method for computing surface integrals. In addition, the authors in [7] showed that the Jacobian can be expressed as the product of the non zero singular values of the Jacobian matrix of the closest point mapping  $P_{\Gamma_0}$ . The benefit of such an expression is that for smooth integrands and smooth curves or surfaces, the accuracy of the discretizations of (3) will depend only on the order of the finite difference scheme used to approximate the Jacobian matrix of  $P_{\Gamma_0}$ .

## 1.1 Computational difficulties near a corner

Both Type I and Type II methods have difficulties resolving singularities from only the values of  $\phi_i$ . In particular, Type II methods using the regularization parameter  $\epsilon$  lead to  $O(\epsilon)$  error for each corner. This error is partially due to the discretization of the Jacobian term. The new approach discussed in this paper does not use the Jacobian term and as such gives a viable approach to handling integrable singularities.

The particular approach described in [6, 7] has specific difficulties in resolving the singularities. Indeed, in a neighborhood of a singular point, the change of variables (5) breaks down. This occurs whenever the signed distance function is not  $C^{1,\alpha}$ ,  $\alpha > 1$ , and when the reach of

the distance function is smaller than the tubular neighborhood  $\{\mathbf{x} : -\epsilon \leq d(\mathbf{x}) \leq \epsilon\}$  (the reach refers to the region near  $\Gamma_0$  where  $d$  is differentiable). In addition, since the expression for the Jacobian  $J$  involves curvatures of level sets, it will be necessary to use one-sided differencing to discretize  $J$  in order to avoid differentiating  $d$  across kinks. Finally, if we consider a corner in two dimensions (see Figure 1) we see that in the convex region enclosed by  $\Gamma_0$  near the corner point, points on an  $\eta$ -level set will not project onto the entire curve  $\Gamma_0$ , whereas points on the  $(-\eta)$ -level set will all project onto  $\Gamma_0$ , leading to a “deficiency” of points coming from one side.

**A characterization of corners and edges via the closest point projection** Let us now use the closest point mapping with distance  $\eta$  more explicitly as  $P_\eta(\mathbf{x}) := \mathbf{x} - \eta \nabla d(\mathbf{x})$ . One way to circumvent this “deficiency” issue is to identify the points on the  $(-\eta)$ -level set that project onto the part of  $\Gamma_0$  that is missed by projecting the points from the  $\eta$  level set. Such points satisfy

$$P_{-\eta}(P_{2\eta}(\mathbf{x})) \neq P_\eta(\mathbf{x}), \eta = d(\mathbf{x}), \quad (6)$$

which states that if we over project  $\mathbf{x}$  by a distance  $2\eta$  and then project the result back by a distance  $\eta$  (in the opposite direction), we are not back at the same point. Points away from the corner on the other hand, i.e. in smooth regions, satisfy  $P_{-\eta}(P_{2\eta}(\mathbf{x})) = P_\eta(\mathbf{x})$ . See Figure 1.

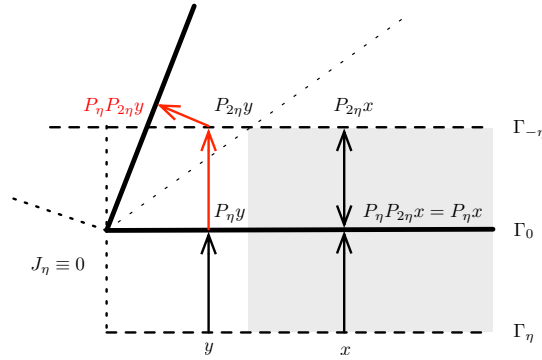


Figure 1: Projection near a corner.

Thus, once we have identified the points that satisfy (6), we count these points twice to compensate for the fact that these points have no corresponding ones on the  $\eta$  level set. This effectively translates into the following correction integral:

$$\int_{\mathbb{R}^2} f(P_\Gamma(\mathbf{x})) \omega(\mathbf{x}) \delta_\epsilon(d(\mathbf{x})) d\mathbf{x},$$

with the weight  $\omega$  defined as

$$\omega(\mathbf{x}) = \begin{cases} 0 & |d(\mathbf{x}) \Delta d(\mathbf{x})| = 1 \\ 2 & P_{-\eta}(P_{2\eta}(\mathbf{x})) = P_\eta(\mathbf{x}), \eta = d(\mathbf{x}) \\ 1 & \text{otherwise.} \end{cases}$$

There are several issues with this approach: the first one is that the modification of the integrand with the weight  $\omega$  leads to a discontinuous integrand. Thus the numerical approximation of the integral will not be able to reach a high order of accuracy. Second, there are numerical difficulties in the implementation of criteria (6): numerically, this requires the use of a threshold, which in turns raises the question of how to choose such a threshold value. Thus, this approach is not suitable for high accuracy and does not provide a seamless implementation.

The purpose of the present work is to give an alternative but related integral formulation that allows the computations of surface integrals where the curve or surface has singular points, and which does not suffer from the issues discussed above. A large advantage of the new approach compared to (3) is that the new formulation does not involve the Jacobian  $J$  and is therefore more convenient to use. Additionally, it provides a mathematical understanding of the relationship between accuracy and how severe a singularity is.

## 2 The extrapolative approach

We now present the new approach which explores the smoothly varying relations among the different level sets of  $\phi$  near  $\Gamma_0$ . In particular, for surfaces having corners, the integration of the nearby parallel surfaces varies smoothly as a function of the distance to the surface  $\Gamma_0$ , except at distance 0 (corresponding to the integral on  $\Gamma_0$ ). Hence, it is possible to use kernels having suitable properties to approximate integration on  $\Gamma_0$  by *extrapolating* integrations defined on other nearby surfaces.

### 2.1 Smooth curves and surfaces

Let  $\phi : \mathbb{R}^n \mapsto \mathbb{R}$ ,  $n \in \mathbb{N}$ , be a Lipschitz function and  $\Gamma_\eta := \{\mathbf{x} : \phi(\mathbf{x}) = \eta\}$  be the  $\eta$ -level set of  $\phi$ . We consider  $\tilde{f} : \mathbb{R}^n \mapsto \mathbb{R}$  to be a Lipschitz function and define  $S$  as

$$S := \int_{\mathbb{R}^n} \tilde{f}(\mathbf{x}) \delta_\epsilon(\phi(\mathbf{x})) |\nabla \phi(\mathbf{x})| d\mathbf{x}. \quad (7)$$

Integrals of the form (7) have been used to approximate  $I_0$  but unlike (3) which coincides exactly with  $I_0$ , we have in general  $S \approx I_0$ . However, under specific conditions which we explain below, it is possible to have  $S = I_0$  or to know precisely how the error between  $S$  and  $I_0$  behaves in terms of  $\epsilon$  (width of the tubular neighborhood around  $\Gamma_0$ ) for example and in terms of a corner or how sharp a cusp is.

We define the one-parameter family of functionals

$$I[\tilde{f}, \phi](\eta) := \int_{\Gamma_\eta} \tilde{f}(\mathbf{x}) dS(\mathbf{x}), \quad (8)$$

which represents the integral of  $\tilde{f}$  over the  $\eta$ -level set of  $\phi$ . It is worth pointing out that in [6, 7], the authors considered a similar approach to construct (3), but their family of functionals was  $F_\eta := \int_{\Gamma_\eta} \tilde{f}(\mathbf{x}) J_\eta(\mathbf{x}) dS(\mathbf{x})$ , where the Jacobian  $J_\eta$  is the same as the Jacobian  $J$  in (3). The purpose of this Jacobian was to ensure the equality  $F_\eta = I_0$  for all  $-\epsilon \leq \eta \leq \epsilon$ . In other words,  $I_0$  was parameterized in terms of the nearby level sets within the tubular neighborhood. Unlike this original approach, (8) is not equal to  $I_0$  for any  $\eta$  since there is no Jacobian term

to compensate for the change in curvature. Now by the coarea formula, we can average over the parameterizations (8) using an averaging kernel  $\delta_\epsilon$  to obtain

$$\int_{-\epsilon}^{\epsilon} \delta_\epsilon(\eta) I[\tilde{f}, \phi](\eta) d\eta = \int_{\mathbb{R}^n} \tilde{f}(\mathbf{x}) \delta_\epsilon(\phi(\mathbf{x})) |\nabla \phi(\mathbf{x})| d\mathbf{x} = S. \quad (9)$$

We then have the following result:

**Theorem 1.** *Suppose that*

1.  $\phi$  is the signed distance function to  $\Gamma_0$ , i.e.  $|\nabla \phi| = 1$ .
2.  $\nabla \tilde{f} \cdot \nabla \phi = 0$  in the viscosity solution sense, meaning that  $\tilde{f}$  is constant along the normals of  $\Gamma_0$  wherever normals are well defined (namely  $\tilde{f}$  is the constant extension of  $f : \Gamma_0 \mapsto \mathbb{R}$  along the normals of  $\Gamma_0$ ).
3.  $\Gamma_\eta$  are closed  $C^2$  hypersurfaces for  $-\epsilon \leq \eta \leq \epsilon$ .

Then for sufficiently small  $\epsilon > 0$  such that  $\Gamma_{\pm\epsilon} \neq \emptyset$ , we have

$$I[\tilde{f}, \phi](\eta) = I_0 + \sum_{i=1}^{d-1} A_i \eta^i,$$

where  $A_i$ ,  $1 \leq i \leq n$  are constants that depend on  $\tilde{f}$  and  $\phi$ .

*Proof.* Let's denote the closest point mapping to  $\Gamma_\eta$  (aka the projection operator onto  $\Gamma_\eta$ ) as  $P_{\Gamma_\eta} : \mathbb{R}^n \mapsto \Gamma_\eta$ . If  $\Gamma_\eta \in C^2(\mathbb{R}^n)$  for all  $-\epsilon \leq \eta \leq \epsilon$ ,  $\epsilon > 0$ , then

$$\begin{aligned} I[\tilde{f}, \phi](\eta) &= \int_{\Gamma_\eta} \tilde{f}(\mathbf{x}) dS(\mathbf{x}) \\ &= \int_{\Gamma_0} \tilde{f}(P_{\Gamma_\eta}(\mathbf{x})) \mathcal{J}_\eta(\mathbf{x}) dS(\mathbf{x}), \end{aligned}$$

where  $\mathcal{J}_\eta$  is the Jacobian that accounts for the change in curvature between  $\Gamma_\eta$  and  $\Gamma_0$ . Using the results from [6],  $\mathcal{J}_\eta$  can be written as  $\mathcal{J}_\eta = 1 + \sum_{i=1}^{n-1} \sigma_i(h) \eta^i$ , where  $\sigma_i(h)$  is the symmetric polynomial in the eigenvalues of the Weingarten map induced by the second fundamental form  $h$  associated to  $\Gamma_\eta$ . Thus we have

$$\begin{aligned} I[\tilde{f}, \phi](\eta) &= \int_{\Gamma_0} \tilde{f}(P_{\Gamma_\eta}(\mathbf{x})) \left( 1 + \sum_{i=1}^{n-1} \sigma_i(h) \eta^i \right) dS(\mathbf{x}) \\ &= \int_{\Gamma_0} \tilde{f}(P_{\Gamma_\eta}(\mathbf{x})) dS(\mathbf{x}) + \sum_{i=1}^{n-1} \eta^i \int_{\Gamma_0} \tilde{f}(P_{\Gamma_\eta}(\mathbf{x})) \sigma_i(h) dS(\mathbf{x}) \\ &= \int_{\Gamma_0} f(x) dS(\mathbf{x}) + \sum_{i=1}^{n-1} \left( \int_{\Gamma_0} \tilde{f}(P_{\Gamma_\eta}(\mathbf{x})) \sigma_i(h) dS(\mathbf{x}) \right) \eta^i \\ &= I_0 + \sum_{i=1}^{n-1} A_i \eta^i, \end{aligned}$$

where  $A_i = \int_{\Gamma_0} \tilde{f}(P_{\Gamma_\eta}(\mathbf{x})) \sigma_i(h) dS(\mathbf{x})$ ,  $1 \leq i \leq n$ , and  $I_0 = \int_{\Gamma_0} \tilde{f}(P_{\Gamma_\eta}(\mathbf{x})) dS(\mathbf{x})$  since  $\tilde{f}$  is constant along the normals to  $\Gamma_0$ , and  $P_{\Gamma_\eta}$  is the orthogonal projection onto  $\Gamma_\eta$ , leading to  $\tilde{f}(P_{\Gamma_\eta}(\mathbf{x})) = f(\mathbf{x})$ , for all  $\mathbf{x} \in \Gamma_0$ .  $\square$

In the dimensions of interest ( $n = 2, 3$ ), the above result states that if  $\Gamma_0$  is  $C^2$ ,  $\tilde{f}$  is constant along the normals of  $\Gamma_0$  and  $\phi$  is the signed distance function to  $\Gamma_0$ , then  $I[\tilde{f}, \phi]$  is linear in  $\eta$  for curves in two dimensions and quadratic in  $\eta$  for surfaces in three dimensions. Therefore, if we average the parameterizations  $I[\tilde{f}, \phi]$  with a kernel  $\delta_\epsilon$  that has enough vanishing moments, the terms in  $\eta$  will vanish and we will be left with  $I_0$ , thus making  $S = I_0$ . The result is stated in the following Corollary:

**Corollary 2.** *Assume that Theorem 1 holds and assume that the averaging kernel  $\delta_\epsilon$  is compactly supported in  $[-\epsilon, \epsilon]$  with  $n - 1$  vanishing moments (where  $n$  is the dimension), namely*

$$\int_{-\infty}^{\infty} \delta_\epsilon(\eta) d\eta = \begin{cases} 1 & p = 0 \\ 0 & 0 < p \leq n - 1, \end{cases}$$

then

$$I_0 = \int_{\Gamma_0} f(x) dS(x) = \int_{\mathbb{R}^n} \tilde{f}(\mathbf{x}) \delta_\epsilon(\phi(\mathbf{x})) d\mathbf{x} = S.$$

*Proof.* Using (9), the result of Theorem (3) and the assumptions on  $\delta_\epsilon$ , we have

$$S = \int_{-\epsilon}^{\epsilon} \delta_\epsilon(\eta) I[\tilde{f}, \phi](\eta) d\eta = \int_{-\epsilon}^{\epsilon} \delta_\epsilon(\eta) \left( I_0 + \sum_{i=1}^{n-1} A_i \eta^i \right) d\eta = I_0 \int_{-\infty}^{\infty} \delta_\epsilon(\eta) d\eta + \sum_{i=1}^{n-1} A_i \int_{-\infty}^{\infty} \delta_\epsilon(\eta) \eta^i d\eta = I_0.$$

$\square$

The main upshot of this result is that if the curve or surface is smooth (i.e.  $C^2$ ), it is possible to construct  $S$  such that it coincides exactly with  $I_0$ . To be more specific, if the kernel  $\delta_\epsilon$  has enough vanishing moments, then  $S = I_0$ . For the dimensions of interest (2 and 3), it is easy to construct kernels with 1 or 2 vanishing moments. For large dimensions, we point out that it might not be easy to construct a kernel with enough vanishing moments to obtain the equality between  $S$  and  $I_0$ , but in that case, the error between  $S$  and  $I_0$  will be related to the number of vanishing moments of  $\delta_\epsilon$ . Thus, the higher the number of vanishing moments, the more accurate the approximation  $S$  will be to  $I_0$ .

Note that in general,  $I[\tilde{f}, \phi]$  may not be a polynomial in  $\eta$ , but as long as  $I[\tilde{f}, \phi]$  has a Taylor expansion about  $\eta = 0$ , the accuracy of using  $S$  to approximate  $I_0$  will be determined by the number of vanishing moments of the kernel  $\delta_\epsilon$ .

There are several implications of this result. First, it is very convenient to use because unlike (3), this formulation does not need the Jacobian term. It is therefore simpler to implement and performs the same as (3) *as long as the kernel is chosen appropriately*. In a way, this can be understood as a trade-off between number of vanishing moments and Jacobian. The Jacobian allows (3) to be exact, but  $S$  can be made exact by using a kernel with enough vanishing moments. Second, this simpler formulation gives a viable approach for approximating integrals over curves and surfaces with singularities.

## 2.2 Curves with corners

In this section, we assume that  $\Gamma_0$  is a closed curve in  $\mathbb{R}^2$  with a corner at  $(x_0, y_0)$ . The purpose of this section is to study the behavior of  $I[\tilde{f}, \phi](\eta)$  as a function of  $\eta$  around  $\eta = 0$  in order to deduce how the error incurred between  $S$  and  $I_0$  depends on the type of singularity (corner or cusp). We describe the corner or cusp as follows: we consider a function  $g : [0, \infty) \mapsto [0, \infty)$  such that  $g(0) = 0$  and for  $x > 0$ ,  $g$  is  $C^2$  with  $g'(0) > 0$ . WLOG, we consider the part of  $\Gamma_0$  around the corner to be defined by the union of the graphs of  $g$  and  $-g$ . In this new coordinate system, the corner is at  $(0, 0)$ . We then parameterize the part of  $\Gamma_0$  that lies above the  $x$ -axis by

$$\gamma(x) := \begin{pmatrix} x \\ g(x) \end{pmatrix},$$

as shown in Figure 2. In this setup, the distance function to  $\Gamma_0$  is differentiable away from the positive  $x$ -axis.

Define the normal to  $\gamma$  by

$$\vec{n}(x) = \frac{1}{\sqrt{1 + g'(x)^2}} \begin{pmatrix} g'(x) \\ -1 \end{pmatrix}$$

and consider the lines

$$L(\eta; x) := \gamma(x) + \eta \vec{n}(x),$$

which correspond to the characteristics of the Eikonal equation that emanates from  $\gamma$  before they intersect the  $x$ -axis. We first find  $\eta$  such that  $L(\eta, x)$  intersects the  $x$ -axis, i.e.

$$\begin{pmatrix} x \\ g(x) \end{pmatrix} + \frac{\eta}{\sqrt{1 + g'(x)^2}} \begin{pmatrix} g'(x) \\ -1 \end{pmatrix} = \begin{pmatrix} X_\eta \\ 0 \end{pmatrix},$$

where  $X_\eta$  is the  $x$ -coordinate of the intersection point between the  $\eta$ -level set and the  $x$ -axis. (See Figure 2).

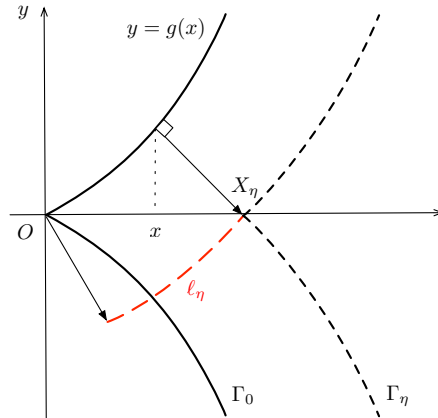


Figure 2: An illustration of a curve with a corner/ cusp and a curve which is  $\eta$  distance away from it.



Using the information from the  $y$ -coordinates in the above vector equation we obtain

$$\eta = g(x)\sqrt{1 + g'(x)^2} := F(x). \quad (10)$$

Thus, the  $\eta(x)$ -level set of the signed distance function to  $\Gamma_0$  has a corner or cusp at  $(X_\eta, 0)$ . Now we estimate the length of the portion of  $\Gamma_0$ , the projection of which to the  $\eta(x)$ -level set is missing, denoted by  $l(x)$  and given by

$$l(x) = \int_0^x \sqrt{1 + g'(\xi)^2} d\xi. \quad (11)$$

If we now look at the integration of  $\tilde{f}$  over a portion of the  $\eta$ -level set of  $d$  above the  $x$ -axis, we are missing the corresponding integral

$$\begin{aligned} l_{\eta(x)}^+[\tilde{f}, d] &= \int_0^{x(\eta)} \tilde{f}(\xi, g(\xi)) \sqrt{1 + g'(\xi)^2} J_\xi d\xi \\ &= \int_0^{x(\eta)} \tilde{f}(\xi, g(\xi)) (1 + \eta \kappa(\xi)) \sqrt{1 + g'(\xi)^2} d\xi \\ &= \int_0^{x(\eta)} \tilde{f}(\xi, g(\xi)) \sqrt{1 + g'(\xi)^2} d\xi + \eta \int_0^{x(\eta)} \tilde{f}(\xi, g(\xi)) \kappa(\xi) \sqrt{1 + g'(\xi)^2} d\xi \\ &= A^+(x(\eta)) + \eta B^+(x(\eta)), \end{aligned}$$

where  $\kappa(\xi)$  is the curvature of  $\Gamma_0$  at the point  $(\xi, g(\xi))$ , and  $x(\eta) = F^{-1}(\eta)$  where  $F$  is given in (10) and  $F$  is invertible around  $x = 0$ . The invertibility of  $F$  is proven in Lemma 5. Away from the corner, the curve is smooth and therefore the error between  $S$  and  $I_0$  is dominated by the effect of the corner. We choose to focus on the corner for  $x \in [0, b]$ ,  $b > 0$ . (See Figure 3).

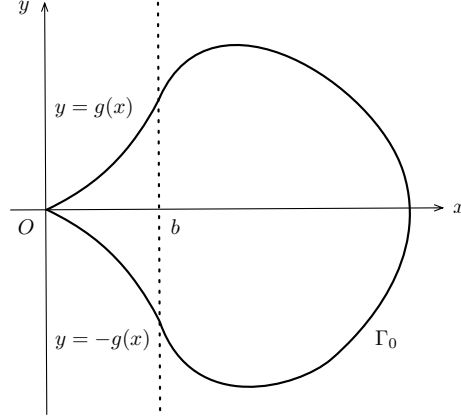


Figure 3: The closed curve  $\Gamma_0$  with a corner at  $(0, 0)$ .

Thus the integral over one side of the corner (above the  $x$ -axis) is

$$\begin{aligned} G_\eta^+ &= \int_0^b \tilde{f}(\xi, g(\xi))(1 + \eta\kappa(\xi))\sqrt{1 + g'(\xi)^2}d\xi \\ &= \int_0^{x(\eta)} \tilde{f}(\xi, g(\xi))(1 + \eta\kappa(\xi))\sqrt{1 + g'(\xi)^2}d\xi + \int_{x(\eta)}^b \tilde{f}(\xi, g(\xi))(1 + \eta\kappa(\xi))\sqrt{1 + g'(\xi)^2}d\xi \\ &= l_\eta^+ + I_\eta^+, \end{aligned}$$

where  $I_\eta^+$  is the integration of  $\tilde{f}$  along the portion of  $\Gamma_\eta$  above the  $x$ -axis. Thus

$$I_\eta^+ = G_\eta^+ - l_\eta^+ = G_\eta^+ - A^+(x(\eta)) - \eta B^+(x(\eta)).$$

The result for the integral along the portion of  $\Gamma_\eta$  below the  $x$ -axis is obtained similarly and thus

$$I_\eta^- = G_\eta^- - l_\eta^- = G_\eta^- - A^-(x(\eta)) - \eta B^-(x(\eta)),$$

with

$$\begin{aligned} A^-(x(\eta)) &= \int_0^{x(\eta)} \tilde{f}(\xi, -g(\xi))\sqrt{1 + g'(\xi)^2}d\xi, \\ B^-(x(\eta)) &= \int_0^{x(\eta)} \tilde{f}(\xi, -g(\xi))\kappa(\xi)\sqrt{1 + g'(\xi)^2}d\xi. \end{aligned}$$

We point out that  $l_\eta^+$  and  $l_\eta^-$  are no longer polynomials in  $\eta$ . WLOG, we assume that  $\Gamma_0$  has only one corner and we denote by  $\mathcal{P}_\eta^+$  and  $\mathcal{P}_\eta^-$  the portion of  $\Gamma_\eta$  above the  $x$ -axis and below the  $x$ -axis respectively. By construction, the term  $G_\eta^+ + G_\eta^- + \int_{\Gamma \setminus (\mathcal{P}_\eta^+ \cup \mathcal{P}_\eta^-)} \tilde{f}(\mathbf{x})dS(\mathbf{x})$  does not have any corner any more. Thus we can apply Theorem 1 and obtain

$$G_\eta^+ + G_\eta^- + \int_{\Gamma \setminus (\mathcal{P}_\eta^+ \cup \mathcal{P}_\eta^-)} \tilde{f}(\mathbf{x})dS(\mathbf{x}) = I_0 + A\eta, \quad A \in \mathbb{R}, \quad (12)$$

which is equivalent to

$$I[\tilde{f}, d](\eta) := I_\eta^+ + I_\eta^- + \int_{\Gamma \setminus (\mathcal{P}_\eta^+ \cup \mathcal{P}_\eta^-)} \tilde{f}(\mathbf{x})dS(\mathbf{x}) = I_0 + A\eta - l_\eta^+ - l_\eta^-. \quad (13)$$

Note that the expression for the constant  $A$  in (12) can be obtained by using the expressions for the constants  $A_i$  given in the proof of Theorem 1.

Not surprisingly, it turns out that there is a fundamental difference in integration of parallel surfaces near a corner and near a cusp on  $\Gamma_0$ .

**Theorem 3.** Consider a curve  $\Gamma_0$  in  $\mathbb{R}^2$  such that  $\Gamma_0$  has a corner at  $(x_0, y_0)$ . Assume  $f \in C^0(\Gamma_0)$  and that the curvature  $\kappa$  is continuous everywhere except at the corner point. Assume that  $g \in C^2([0, \infty))$  with  $g(0) = 0$  and for  $x > 0$ ,  $g'(x) > 0$ , such that the corner is modeled by the graphs of  $g$  and  $-g$ . In this new coordinate system, the corner is at  $(0, 0)$ . Suppose also that the averaging kernel  $\delta_\epsilon$  is compactly supported in  $[-\epsilon, \epsilon]$  with  $m$  vanishing moments. Define  $F : [0, \infty) \mapsto [0, \infty)$  as  $F(x) = g(x)\sqrt{1 + g'(x)^2}$ . If  $F(x) = ax^p + o(x^p)$  as  $x \rightarrow 0$  ( $a \in \mathbb{R} \setminus \{0\}$ ) with  $p \in \mathbb{N}$ , and if

$$\delta_\epsilon(\eta) = O(\epsilon^{-k})$$

as  $\eta \rightarrow 0$ , ( $k \in \mathbb{N}$ ), then

$$|S - I_0| = \begin{cases} O(\epsilon^{2+m-k}) & p = 1 \text{ (corner)} \\ O(\epsilon^{1+\frac{1}{p}-k}) & p \geq 2 \text{ (cusp)} \end{cases},$$

for small  $\epsilon > 0$ .

Note that the number of vanishing moments of the kernel  $\delta_\epsilon$  only plays a role in the case of a corner. For cusps, it is necessary to construct a different class of kernels that integrate to zero when multiplied by fractional powers of  $\eta$ .

### 3 Proof of Theorem 3

We start with two technical lemmas that are needed to complete the proof of Theorem 3 and then give the proof of Theorem 3.

**Lemma 4.** Suppose  $p \in \mathbb{N}$ , and assume that  $k : \mathbb{R} \mapsto \mathbb{R}$  is a function that satisfies the condition  $\lim_{x \rightarrow 0} \frac{k(x)}{x^p} = 0$ . Assume also that  $x \mapsto \frac{k(x)}{x^p}$  is an increasing function of  $x$  on  $\mathbb{R}^+$  and a decreasing function of  $x$  on  $\mathbb{R}^-$ . Then if  $\alpha_p > 0$ , the series

$$\sum_{n=0}^{\infty} \binom{\frac{1}{p}}{n} \left( \frac{k(x)}{\alpha_p x^p} \right)^n$$

is uniformly convergent for  $|x| < r$  for some  $r > 0$ .

*Proof.* The assumption  $\lim_{x \rightarrow 0} \frac{k(x)}{x^p} = 0$  states that  $k$  goes to zero faster than  $x^p$ , leading to the quotient  $\left| \frac{k(x)}{x^p} \right|$  being eventually less than  $\alpha_p$  as  $x \rightarrow 0$ , and thus there exists  $r > 0$  such that  $\left| \frac{k(x)}{\alpha_p x^p} \right| < 1$  when  $|x| < r$ . Thus, since

$$\left| \binom{\frac{1}{p}}{n} \right| \left| \frac{k(x)}{\alpha_p x^p} \right|^n \leq \left| \frac{k(x)}{\alpha_p x^p} \right|^n$$

the series is convergent for  $|x| < r$ . The last inequality comes from the fact that the sequence  $\left| \binom{\frac{1}{p}}{n} \right|$  is decreasing in  $n$ , which we prove at the end. Now we want to show that the series is uniformly convergent in that interval. Pick  $0 < \rho < r$ . Then for  $|x| < \rho < r$ , we have

$$\left| \frac{k(x)}{x^p} \right| < \left| \frac{k(\rho)}{\rho^p} \right| < \alpha_p.$$

Thus we have

$$\left| \binom{\frac{1}{p}}{n} \left( \frac{k(x)}{\alpha_p x^p} \right)^n \right| < \left| \binom{\frac{1}{p}}{n} \frac{k(\rho)}{\alpha_p \rho^p} \right|^n := \left| \binom{\frac{1}{p}}{n} \right| \zeta^n \leq \zeta^n,$$

with  $|\zeta| < 1$ . Consequently, the series  $\sum_{n=0}^{\infty} \left| \binom{\frac{1}{p}}{n} \right| \zeta^n$  converges. Thus by the Weierstrass M-test, it follows that the series converges uniformly for  $|x| < \rho$ . Since  $\rho$  is arbitrary in  $(0, r)$ , the series converges uniformly for  $|x| < r$ .

We now show that the sequence  $\left| \left( \frac{1}{p} \right)_n \right|$  is decreasing in  $n$ . Let  $u_n^p := \left| \left( \frac{1}{p} \right)_n \right|$ . For  $p = 1$ , we have  $u_0^1 = u_1^1 = 1$  and  $u_n^1 = 0$  for  $n \geq 2$ . Thus,  $\forall n \geq 0, u_n^1 \leq 1$ . Now, consider  $p \geq 2$ . By definition of the sequence, we have

$$\forall k \in \mathbb{N}, \left( \frac{1}{p} \right)_{2k} = -u_{2k}^p \leq 0, u_{2k-1}^p \geq 0.$$

For  $k \geq 1$ , we have

$$\begin{aligned} u_{2k+1}^p - u_{2k}^p &= \frac{\frac{1}{p}(\frac{1}{p}-1)(\frac{1}{p}-2)\cdots(\frac{1}{p}-2k)}{(2k+1)!} - \frac{-\frac{1}{p}(\frac{1}{p}-1)(\frac{1}{p}-2)\cdots(\frac{1}{p}-2k+1)}{(2k)!} \\ &= \frac{\frac{1}{p}(\frac{1}{p}-1)(\frac{1}{p}-2)\cdots(\frac{1}{p}-2k+1)}{(2k)!} \left( 1 + \frac{\frac{1}{p}-2k}{2k+1} \right), \\ &= \frac{\frac{1}{p}(\frac{1}{p}-1)(\frac{1}{p}-2)\cdots(\frac{1}{p}-2k+1)}{(2k)!} \left( \frac{1+\frac{1}{p}}{2k+1} \right) < 0, \end{aligned}$$

since the numerator of the first fraction is the product of an even number of terms, and thus is negative.

Similarly, for  $k \geq 1$ , we have

$$u_{2k}^p - u_{2k-1}^p = \frac{\frac{1}{p}(\frac{1}{p}-1)(\frac{1}{p}-2)\cdots(\frac{1}{p}-2k+2)}{(2k-1)!} \left( -\frac{\frac{1}{p}+1}{2k} \right) < 0,$$

since the numerator in the first fraction is the product of an odd number of terms, which is positive. Thus

$$\forall n \geq 1, p \geq 1, u_{n+1}^p - u_n^p \leq 0.$$

Since  $u_0^p = 1, \forall p \geq 1$  and  $u_1^p = \frac{1}{p}, \forall p \geq 1$ , it follows that

$$\forall n \geq 0, p \geq 1, u_{n+1}^p - u_n^p \leq 0.$$

Thus the sequence is decreasing and bounded above by its first term, which is 1.

□

**Lemma 5.** Assume that  $g \in C^2([0, \infty))$  such that  $g(0) = 0$  and for  $x > 0$ ,  $g'(x) > 0$ . Let  $p \in \mathbb{N}$  such that  $g^{(\nu)}(0) = 0$  for  $0 \leq \nu < p$ , and let  $F : [0, \infty) \mapsto [0, \infty)$  be defined as  $F(x) = g(x)\sqrt{1 + g'(x)^2}$ . Then locally around  $x = 0$ ,  $F$  is invertible and  $F(x) = ax^p + o(x^p)$  as  $x \rightarrow 0$  ( $a \in \mathbb{R} \setminus \{0\}$ ) with  $p \in \mathbb{N}$ , and

$$x(\eta) = F^{-1}(\eta) = \left( \frac{\eta}{a} \right)^{\frac{1}{p}} + o(\eta^{\frac{1}{p}})$$

as  $\eta \rightarrow 0$ .

*Proof.* Since  $g \in C^2([0, \infty))$ , then  $F(x) = g(x)\sqrt{1 + g'(x)^2}$  is in  $C^1([0, \infty))$ , with

$$F'(x) = \frac{g'(x)(1 + g'(x)^2) + g(x)g'(x)g''(x)}{\sqrt{1 + g'(x)^2}} = \frac{g'(x)}{\sqrt{1 + g'(x)^2}}(1 + g'(x)^2 + g(x)g''(x)).$$

- Case 1. Corner case: suppose  $g'(0) > 0$ . Then  $F'(0) = \frac{g'(0)(1+g'(0)^2)}{\sqrt{1+g'(0)^2}} > 0$ . Since  $F'$  is continuous on  $[0, \infty)$ , one can find a neighborhood of  $x = 0$ ,  $[0, \nu)$  (for some  $\nu > 0$ ), such that for all  $x \in [0, \nu)$ , we have  $F'(x) > 0$ . Thus,  $F$  is strictly increasing on  $[0, \nu)$  and therefore invertible on  $[0, \nu)$ , i.e.

$$\forall x \in [0, \nu), x = F^{-1}(\eta)$$

with  $F^{-1}(0) = 0$  (since  $g(0) = 0 \Rightarrow F(0) = 0$ ). Since  $F \in C^2([0, \infty))$  with  $F'(0) > 0$ , it follows that  $F$  has can be written as

$$F(x) = a_1x + a_2x^2 + g(x),$$

where  $a_1 = F'(0) > 0$ , and  $\lim_{x \rightarrow 0} \frac{g(x)}{x^2} = 0$ . Thus  $F(x) = a_1x + o(x)$  as  $x \rightarrow 0$  with  $a_1 \neq 0$ . Let us look for its local inverse around  $x = 0$ ,  $F^{-1}$ , as

$$F^{-1}(\eta) = b_1\eta + h(\eta), \tag{14}$$

such that  $\lim_{\eta \rightarrow 0} \frac{h(\eta)}{\eta} = 0$ . Then using  $F^{-1}(F(x)) = x$  for  $x \in [0, \nu)$ , we obtain

$$\begin{aligned} F^{-1}(F(x)) &= F^{-1}(a_1x + a_2x^2 + g(x)) \\ &= b_1(a_1x + a_2x^2 + g(x)) + h(a_1x + a_2x^2 + g(x)) \\ &= a_1b_1x + b_1a_2x^2 + b_1g(x) + h(a_1x + a_2x^2 + g(x)) \\ &= a_1b_1x + R(x), \end{aligned}$$

where  $R(x) = b_1a_2x^2 + b_1g(x) + h(a_1x + a_2x^2 + g(x))$ . If we choose  $b_1 = \frac{1}{a_1}$ , then for  $x \in [0, \nu)$  we have

$$F^{-1}(F(x)) = x + R(x).$$

Now  $F^{-1}$  is the correct inverse if  $R(x) = 0$  but we cannot know what  $R$  is since we do not have an expression for  $g$  and  $h$ . Nevertheless, asymptotically around  $x = 0$ ,  $R$  needs to satisfy  $\lim_{x \rightarrow 0} \frac{R(x)}{x} = 0$ . Let us then calculate this limit:

$$\begin{aligned} \lim_{x \rightarrow 0} \frac{R(x)}{x} &= \lim_{x \rightarrow 0} \frac{b_1a_2x^2 + b_1g(x) + h(a_1x + a_2x^2 + g(x))}{x} \\ &= b_1a_2 \lim_{x \rightarrow 0} x + b_1 \lim_{x \rightarrow 0} \frac{g(x)}{x} + \lim_{x \rightarrow 0} \frac{h(a_1x + a_2x^2 + g(x))}{x} \\ &= 0, \end{aligned}$$

since  $\lim_{x \rightarrow 0} \frac{g(x)}{x^2} = 0 \Rightarrow \lim_{x \rightarrow 0} \frac{g(x)}{x} = 0$  and  $\lim_{x \rightarrow 0} \frac{h(a_1x + a_2x^2 + g(x))}{x} = \lim_{y \rightarrow 0} \frac{h(y)}{y} = 0$  with  $y = a_1x + a_2x^2 + g(x) = a_1x + o(x) \rightarrow_{x \rightarrow 0} 0$ . Thus if the inverse  $F^{-1}$  is of the form (14), we have the correct asymptotic behavior for  $F^{-1} \circ F$ . By the unicity of the inverse, it follows that necessarily around  $\eta = 0$  we have

$$F^{-1}(\eta) = \frac{\eta}{a_1} + h(\eta),$$

with  $\lim_{\eta \rightarrow 0} \frac{h(\eta)}{\eta} = 0$ .

- Case 2: Cusp case: suppose  $g^{(\nu)}(0) = 0$  for  $0 \leq \nu < p$  ( $p \in \mathbb{N}, p \geq 2$ ). Then  $F'(0) = 0$ . First, let's show that  $F$  is invertible and to do so, we will show that  $F'(x) > 0$  on an interval  $(0, \mu)$ , for some  $\mu > 0$ . We first point out that  $g'(0) = 0$  together with  $g'(x) > 0$  for  $x > 0$  and the continuity of  $g'$  implies that  $g'$  is increasing on an interval  $(0, \mu)$  for some  $\mu > 0$ , meaning that close to  $x = 0$ ,  $g$  is concave up, i.e.

$$\forall x \in (0, \mu), g''(x) > 0.$$

It follows that on  $(0, \mu)$ ,  $F'(x) > 0$ . The reason for this statement comes from the fact that  $F'(x) = 0 \Leftrightarrow 1 + g'(x)^2 = -g(x)g''(x)$ , which can only occur whenever  $g''(x) \leq 0$ , since  $1 + g'(x)^2 > 0$  for all  $x$ , and  $g(x) \geq 0$ . Thus since  $g''(x) > 0$  on  $(0, \mu)$ , it follows that  $F'(x) > 0$  and thus  $F$  is invertible on  $(0, \mu)$ . Now since  $g \in C^2([0, \infty))$  with  $g(0) = g'(0) = 0$ , it follows that  $F$  is  $C^1([0, \infty))$  with  $F(0) = F'(0) = 0$ . Let us assume that we can write  $F$  as follows

$$F(x) = \alpha_p x^p + k(x),$$

with  $\alpha_p > 0$ ,  $\lim_{x \rightarrow 0} \frac{k(x)}{x^p} = 0$  and such that  $x \mapsto \frac{k(x)}{x^p}$  is an increasing function of  $x$  on  $\mathbb{R}^+$  and a decreasing function of  $x$  on  $\mathbb{R}^-$ . We then look for its local inverse  $F^{-1}$  as

$$F^{-1}(\eta) = \beta_1 \eta^{\frac{1}{p}} + l(\eta),$$

such that  $\lim_{\eta \rightarrow 0} \frac{l(\eta)}{\eta^{\frac{1}{p}}} = 0$ . Using  $F^{-1}(F(x)) = x$  on  $(0, \mu)$ , we obtain

$$\begin{aligned} F^{-1}(F(x)) &= \beta_1 F(x)^{\frac{1}{p}} + l(F(x)) \\ &= \beta_1 (\alpha_p x^p + k(x))^{\frac{1}{p}} + l(\alpha_p x^p + k(x)) \\ &= \beta_1 \alpha_p^{\frac{1}{p}} x \sum_{n=0}^{\infty} \binom{\frac{1}{p}}{n} \left( \frac{k(x)}{\alpha_p x^p} \right)^n + l(\alpha_p x^p + k(x)) \\ &= \beta_1 \alpha_p^{\frac{1}{p}} x + T(x), \end{aligned}$$

where  $T(x) = \beta_1 \alpha_p^{\frac{1}{p}} x \sum_{n=1}^{\infty} \binom{\frac{1}{p}}{n} \left( \frac{k(x)}{\alpha_p x^p} \right)^n + l(\alpha_p x^p + k(x))$ . If we choose  $\beta_1 = \alpha_p^{-\frac{1}{p}}$ , then we have  $F^{-1}(F(x)) = x + T(x)$ . It remains to show that this gives the correct asymptotic behavior at  $x = 0$ , namely that  $\lim_{x \rightarrow 0} \frac{T(x)}{x} = 0$ .

$$\begin{aligned} \lim_{x \rightarrow 0} \frac{T(x)}{x} &= \lim_{x \rightarrow 0} \frac{\beta_1 \alpha_p^{\frac{1}{p}} x \sum_{n=1}^{\infty} \binom{\frac{1}{p}}{n} \left( \frac{k(x)}{\alpha_p x^p} \right)^n + l(\alpha_p x^p + k(x))}{x} \\ &= \beta_1 \alpha_p^{\frac{1}{p}} \lim_{x \rightarrow 0} \sum_{n=1}^{\infty} \binom{\frac{1}{p}}{n} \left( \frac{k(x)}{\alpha_p x^p} \right)^n + \lim_{x \rightarrow 0} \frac{l(\alpha_p x^p + k(x))}{x} \\ &= \beta_1 \alpha_p^{\frac{1}{p}} \sum_{n=1}^{\infty} \binom{\frac{1}{p}}{n} \frac{1}{\alpha_p^n} \lim_{x \rightarrow 0} \left( \frac{k(x)}{x^p} \right)^n + \lim_{x \rightarrow 0} \frac{l(\alpha_p x^p + k(x))}{x}, \end{aligned}$$

where we have used the uniform convergence of the series  $\sum_{n=1}^{\infty} \binom{\frac{1}{p}}{n} \left( \frac{k(x)}{\alpha_p x^p} \right)^n$  to interchange the sum and the limit by Lemma 4. Thus, since  $\lim_{x \rightarrow 0} \frac{k(x)}{x^p} = 0$  it follows that for

all  $n \geq 1$ , we have  $\lim_{x \rightarrow 0} \left( \frac{k(x)}{x^p} \right)^n = 0$ . Additionally,  $\lim_{x \rightarrow 0} \frac{l(\alpha_p x^p + k(x))}{x} = \lim_{y \rightarrow 0} \frac{l(y)}{y^{\frac{1}{p}}} = 0$

with  $y = \alpha_p x^p + k(x) = O(x^p) \Rightarrow x = O(y^{\frac{1}{p}})$ . Therefore  $\lim_{x \rightarrow 0} \frac{T(x)}{x} = 0$ , hence leading to the desired asymptotic behavior. Since the inverse is unique, it follows that asymptotically around  $\eta = 0$  we have

$$F^{-1}(\eta) = \left( \frac{\eta}{\alpha_p} \right)^{\frac{1}{p}} + l(\eta),$$

where  $\lim_{\eta \rightarrow 0} \frac{l(\eta)}{\eta^{\frac{1}{p}}} = 0$ .

□

*Proof.* (of Theorem 3). As shown earlier we have for  $\eta > 0$ ,

$$l_{\eta}^{\pm} = A^{\pm}(x(\eta)) + \eta B^{\pm}(x(\eta)).$$

Since  $f$  is continuous and  $\kappa$  is continuous everywhere except at the corner point, we have  $f(\xi, \pm g(\xi))\sqrt{1 + g'(\xi)^2} = O(1)$  and  $f(\xi, \pm g(\xi))\kappa(\xi)\sqrt{1 + g'(\xi)^2} = O(1)$  as  $x \rightarrow 0$ . Thus

$$\begin{aligned} A^{\pm}(x(\eta)) &= \int_0^{x(\eta)} f(\xi, \pm g(\xi))\sqrt{1 + g'(\xi)^2} d\xi \\ &= O(\eta^{\frac{1}{p}}) \text{ as } \eta \rightarrow 0^+, \end{aligned}$$

and

$$\begin{aligned} B^{\pm}(x(\eta)) &= \int_0^{x(\eta)} f(\xi, \pm g(\xi))\kappa(\xi)\sqrt{1 + g'(\xi)^2} d\xi \\ &= O(\eta^{\frac{1}{p}}) \text{ as } \eta \rightarrow 0^+ \end{aligned}$$

by using Lemma 5. Thus

$$l_{\eta}^{\pm} = O(\eta^{\frac{1}{p}}) \text{ as } \eta \rightarrow 0^+.$$

Therefore, using (13), we have

$$I[\tilde{f}, d](\eta) = I_0 + O(\eta^{\frac{1}{p}}) \text{ as } \eta \rightarrow 0^+.$$

For  $\eta < 0$ , since everything is smooth on that side, we can apply Theorem 1 to obtain

$$I[\tilde{f}, d](\eta) = I_0 + O(\eta) \text{ as } \eta \rightarrow 0^-.$$

For  $p = 1$ , we have

$$\begin{aligned} S &= \int_{\epsilon}^{\epsilon} I[\tilde{f}, d](\eta) \delta_{\epsilon}(\eta) d\eta \\ &= \int_{-\epsilon}^{\epsilon} I_0 \delta_{\epsilon}(\eta) d\eta + O\left(\int_{-\epsilon}^{\epsilon} \eta \delta_{\epsilon}(\eta) d\eta\right) \\ &= I_0 + O\left(\int_{-\epsilon}^{\epsilon} \eta \delta_{\epsilon}(\eta) d\eta\right). \end{aligned}$$

In this case,  $I[\tilde{f}, d](\eta)$  only contains integer powers of  $\eta$  (Taylor series). It follows that since  $\delta_\epsilon$  has  $m$  vanishing moments,

$$\begin{aligned} S &= I_0 + O\left(\int_{-\epsilon}^{\epsilon} \eta^{m+1} \delta_\epsilon(\eta) d\eta\right) \\ &= I_0 + O\left(\epsilon^{-k} \int_{-\epsilon}^{\epsilon} \eta^{m+1} d\eta\right) \\ &= I_0 + O(\epsilon^{m+2-k}). \end{aligned}$$

For  $p \geq 2$ , we have

$$\begin{aligned} S &= \int_{-\epsilon}^{\epsilon} I[\tilde{f}, d](\eta) \delta_\epsilon(\eta) d\eta \\ &= \int_{-\epsilon}^0 I[\tilde{f}, d](\eta) \delta_\epsilon(\eta) d\eta + \int_0^{\epsilon} I[\tilde{f}, d](\eta) \delta_\epsilon(\eta) d\eta \\ &= \int_{-\epsilon}^{\epsilon} I_0 \delta_\epsilon(\eta) d\eta + O\left(\int_{-\epsilon}^0 \eta \delta_\epsilon(\eta) d\eta\right) + O\left(\int_0^{\epsilon} \eta^{\frac{1}{p}} \delta_\epsilon(\eta) d\eta\right) \\ &= I_0 + O\left(\epsilon^{-k} \int_{-\epsilon}^0 \eta d\eta\right) + O\left(\epsilon^{-k} \int_0^{\epsilon} \eta^{\frac{1}{p}} d\eta\right) \\ &= I_0 + O(\epsilon^{-k+2}) + O(\epsilon^{-k+\frac{1}{p}+1}) \\ &= I_0 + O(\epsilon^{1+\frac{1}{p}-k}). \end{aligned}$$

□

## 4 Numerical simulations

In this section, we present a few numerical computations aiming at demonstrating the unique properties of the proposed approach to surface integrals using implicit representations. These properties include:

1. High order approximations of smooth or piecewise smooth interfaces with the use of sufficiently regular level set functions.
2. Analytically exact integrals and highly accurate numerical approximations with the help of a sufficiently regular level set function and constant-in-normal extensions of the integrands.
3. The potential in computing singular integrals using uniform Cartesian grids.

These properties are the consequences of the use of special averaging kernels. The numerical computations presented in this section will involve the following kernels, constructed in [2]:

- A  $C^\infty$  kernel with one vanishing moment:

$$\begin{aligned} \delta_{\infty,1}(r) &:= \exp\left(\frac{2}{(2r-1)^2-1}\right) (ar+b) \chi_{[0,1]}(r), \\ a &= -261.5195892865372, b = 145.7876577089403. \end{aligned}$$



- A  $C^\infty$  kernel with one vanishing moment:

$$\delta_{\rho,\infty,1}(r) := \exp\left(\frac{1}{2(r^2 - 1)}\right) (ar + b)\chi_{[\rho,1]}(r),$$

$$a = -759.2781934172483, b = 446.2604260472818.$$

This kernel is designed specifically for integrands with an integrable singularity. The support of the kernel, which is  $\rho$  away from the singularity, is constructed to mitigate the effect of the singularity. In the following computations,  $\rho$  is taken to be 0.1.

- A  $C^\infty$  kernel with two vanishing moments :

$$\delta_{\infty,2}(r) := \exp\left(\frac{2}{(2r - 1)^2 - 1}\right) (ar^2 + br + c)\chi_{[0,1]}(r),$$

$$a = 3196.1015220946833, b = -3457.6211113812255, c = 852.9832518883903.$$

**Example 6.** In this example, we compute the length of the circle  $x^2 + y^2 = r_0^2$ , defined as the zero level set of the function  $\phi(x, y) = x^2 + y^2 - r_0^2$  using

$$S_N := \sum_{i,j} \epsilon^{-1} \delta(\epsilon^{-1} \phi_{i,j}) |\nabla \phi_{i,j}| h^2.$$

In Table 1, we present our computations with radius  $r_0 = 0.501$ , and  $\epsilon = 2h^{1/2}$  with  $h = 2/N$ , where  $N$  is the number of grid points along one coordinate direction. The theoretical convergence rate for  $\delta_{\infty,1}$  with  $\epsilon = 2h^{1/2}$  is 1 while that of  $\delta_{\infty,2}$  is 1.5. We point out that with the same  $\epsilon$  at  $N = 100$ , if we used the signed distance function,  $\phi(x, y) = \sqrt{x^2 + y^2} - r_0$  to the same circle, the relative error using  $\delta_{\infty,1}$  would be  $2.31890e - 08$ . This reflects the property of the integral  $I[\tilde{f} \equiv 1, \phi](\eta)$ , defined in (8), as a function of  $\eta$ .

Table 1: Relative error in computing the circumference of a circle using a non-distance level set function.

	N=100	200	400	800	1600	3200
Rel. err. $w_{\infty,1}$	2.19034e-02	1.22417e-02	6.72509e-03	3.61084e-03	1.90462e-03	9.90744e-04
Order		0.8	0.9	0.9	0.9	0.9
Rel. err. $w_{\infty,2}$	2.99384e-03	1.53839e-03	6.34199e-04	2.55519e-04	9.96251e-05	3.78689e-05
Order		1.0	1.3	1.3	1.4	1.4

**Example 7.** In this example, we compute the length of the black curve shown in Figure 4, which has four cusps. The curve  $\Gamma_0$  is defined by the four quarter of circles with radius  $r_0 = 0.75$ , centered respectively as  $(r_0, 0)$ ,  $(-r_0, 0)$ ,  $(0, r_0)$  and  $(0, -r_0)$ .

The length is computed by the formula

$$S_N^+ := \sum_{i,j,k} \epsilon^{-1} \delta_{\infty,1}(\epsilon^{-1} d_{i,j}) h^2$$

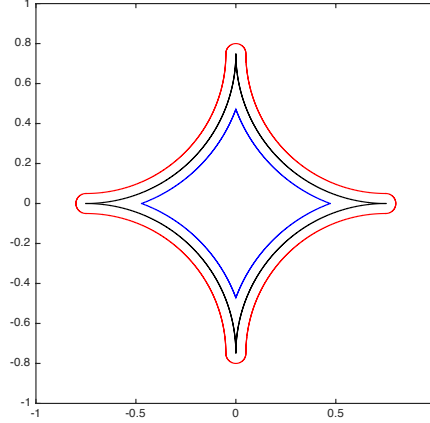


Figure 4: Cusp

using  $\epsilon = 0.05$ . The relative errors are tabulated in Table 2. The convergence in this example is actually exponential, namely the error decays like  $\alpha^N$ , with  $0 < \alpha < 1$ . In this example,  $\alpha \approx 0.9954$ . Figure 7 shows the exponential convergence rate. Here  $d_{i,j}$  denotes the value of the signed distance function to  $\Gamma_0$  at the point  $(x_i, y_j)$ . In the computations, the sign of the signed distance function to  $\Gamma_0$  is designated to be negative inside the enclosed region. Note that the level sets of  $d$  in the region  $\{d > 0\}$  are continuously differentiable. As the analysis in the above section shows, computations performed in  $\{d < 0\}$  using

$$S_N^- := \sum_{i,j,k} \epsilon^{-1} \delta_{\infty,1}(-\epsilon^{-1} d_{i,j}) h^2,$$

will not yield accurate approximations due to the singularity of  $I[\tilde{f} \equiv 1, \phi](\eta)$  near  $\eta = 0^-$ .

Table 2: Relative errors in computing the length of the black curve, containing four cusps, in Figure 4.

$w_{\infty,1}$	N=100	200	400	800	1600	3200
Rel. error $S_N$	7.04018e-3	6.63514e-4	4.43853e-5	4.45564e-7	5.84085e-9	3.74043e-12
Order		3.4	3.9	6.6	6.3	10.6

In Table 3, we present the numerical errors computed by  $\tilde{S}_N^-$  to approximate the length of the interface which is 0.05 distance away from the black curve shown in Figure 4

$$\tilde{S}_N^- := \sum_{i,j,k} \epsilon^{-1} \delta_{\infty,1}(-\epsilon^{-1}(d_{i,j} + 0.05)) h^2.$$

**Example 8.** We compute the surface area of  $\phi(x, y, z) := |x| + |y| + |z| = r_0$  (graphed in Figure 6) with  $r_0 = 0.65$  by the following sum

$$S_N := \sum_{i,j,k} \epsilon^{-1} \delta_{\infty,2}(\epsilon^{-1} \phi_{i,j,k}) |\nabla \phi_{i,j,k}| h^3,$$

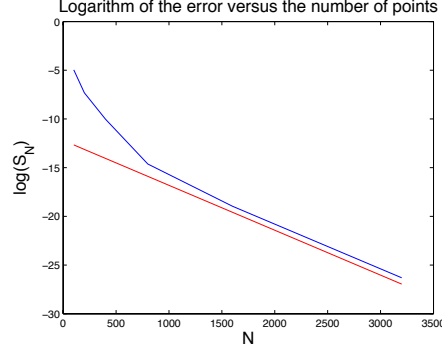


Figure 5: Logarithm of the error versus the number of points for Example 7. This figure illustrates the fact that the convergence rate of the simulation the results of which are tabulated in Table 2 is exponential. In this simulation, the error scales as  $\alpha^N$  with  $\alpha \approx 0.9954$ . The blue line is the logarithm of the computed errors, while the red line is the logarithm of  $\alpha^N$ .

Table 3: Relative errors in computing the length of the blue curve, containing four corners, in Figure 4. The theoretical convergence rate for this simulation is 2.0.

$w_{\infty,2}$	$\epsilon$	N=100	200	400	800	1600	3200
Rel. error $S_N$	$3.4N^{-2/3}$	1.64925e-02	8.63529e-03	2.98334e-03	1.08381e-03	3.34617e-04	9.79520e-05
Order			0.9	1.5	1.5	1.7	1.8

where  $|\nabla\phi_{i,j,k}| \equiv \sqrt{3}$ .

The relative errors with  $\epsilon = 0.1$  and a few values of  $h = 1/N$  are presented in Table 4. The convergence rate in this simulation is also exponential and is illustrated in Figure 7. The point of this example is to demonstrate that the proposed approach is able to compute high order approximations of surface integrals, in the case where the surface and the embedding level set function are only piecewise smooth. This capability is not seen in other existing level set methods.

Table 4: Relative error in computing the surface area of an  $\ell_1$ -ball.

	N=100	200	400	800
Rel. error	5.87232e-1	2.63126e-2	8.19894e-4	5.23091e-6
Order		4.5	5.0	7.3

**Example 9.** In this example, we compute the line integral of a function that has an integrable singularity at a corner of the interface. Let  $\phi^{(1)}(x, y) := |x| + |y| - 1$ ,  $\phi^{(2)} = (|x| + |y|)^2 - 1$  and  $f(r) = 1/\sqrt{r}$ . We define the interface  $\Gamma_0 := \{\phi = 0\}$  and we approximate the integral

$$\int_{\Gamma_0} f(\sqrt{x^2 + (y+1)^2}) dS(x, y)$$

by

$$S_N^{(\ell)} := \sum_{i,j} f(\sqrt{x_i^2 + (y_j + 1)^2}) \epsilon^{-1} \delta(\epsilon^{-1} \phi_{i,j}^{(\ell)}) |\nabla \phi_{i,j}^{(\ell)}| h^2,$$

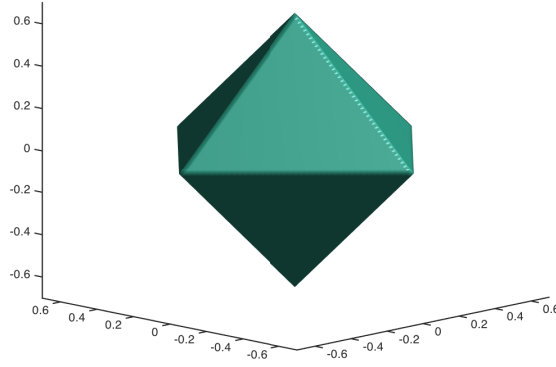


Figure 6: Surface area of  $|x| + |y| + |z| = r_0$  computed in Example 8.

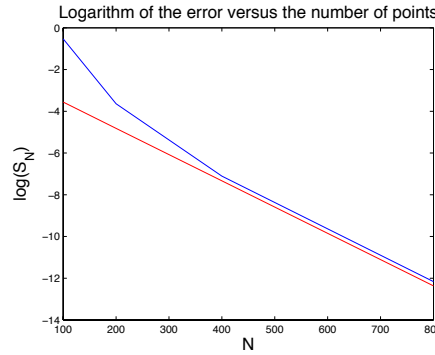


Figure 7: Logarithm of the error versus the number of points for Example 8. This figure illustrates the fact that the convergence rate of the simulation the results of which are tabulated in Table 4 is exponential. In this simulation, the error scales as  $\alpha^N$  with  $\alpha \approx 0.9875$ . The blue line is the logarithm of the computed errors, while the red line is the logarithm of  $\alpha^N$ .

where  $\delta$  is one of the kernels described above.

This is an example that suggests the potential of the proposed extrapolative approach in computing integrands involving integrable singularities. For integration of singularities such as  $1/\sqrt{x}$  in the interval  $[0, 1]$ , one typically needs to require that the step size  $h = h(x)$  decreases sufficiently fast as  $x$  tends to 0, otherwise, the resulting quadrature will have a significant drop in the order of accuracy. The level set function  $\phi^{(2)}$  is proportional to the squared distance to the interface  $\Gamma_0$  (the zero level set of  $\phi^{(2)}$ ), and when discretized with a uniform grid, one has effectively an adaptive meshing with quadratic refinement in the step size in the direction normal to the interface. Of course, in the tangential direction, no such automatic mesh refinement is created near the singularity. In Table 5, we present numerical errors of our computations for such problems using  $\delta = \delta_{\rho, \infty, 1}$  and  $a_1 \approx 8.45$ , where the constant  $a_1$  adjusts the value of  $\epsilon$  to the lowest grid. The analysis of our approach to this type of singular integrals is the subject of another paper.

Table 5: Relative errors in the computation of an singular integral.

Ker= $w_{\delta,\infty,1}$	$\epsilon$	N=200	400	800	1600	3200
Rel. err. $\phi^{(1)}$	$a_1 N^{-0.95}$	4.90965e-02	3.07270e-02	4.44569e-03	7.55996e-03	2.62123e-02
Order			0.7	2.8	-0.8	-1.8
Rel. err. $\phi^{(2)}$	$\sqrt{a_1} N^{-0.475}$	1.83031e-02	1.07425e-02	5.52434e-03	2.11137e-03	6.33622e-05
Order			0.8	1.0	1.4	5.1

## 5 Discussion

In this section, we compare this new approach with the original KTT approach constructed in [6] and discuss the potentials of the extrapolative approach for hypersurfaces with singularities. For smooth hypersurfaces, the original and the extrapolative approach both yield an exact result, namely the volume integral coincide exactly with the hypersurface integral one wishes to compute. However, exactness is not obtained the same way. The original approach needs a Jacobian term in the integrand: this Jacobian corrects for the change in curvature incurred when one moves away from the hypersurface (namely the zero level set of the level set function). The extrapolative approach does not have a Jacobian but instead requires the approximation of the Dirac delta function to have at least  $n - 1$  vanishing moments, where  $n$  is the dimension. While the choice of the method is ultimately up to the practitioner, we believe it is easier to use the original approach on smooth hypersurfaces since (a) the Jacobian is easy to compute using the singular values of the Jacobian matrix of the closest point mapping (see [7]), and (b) there is no need to construct kernels with large numbers of vanishing moments, other than accuracy gain.

On the other hand, while the original approach suffers from low accuracy when used on hypersurfaces with singularities, the extrapolative approach is better suited for such cases. That said, we point out that for hypersurfaces with singularities, neither one of these two approaches will yield an integral formulation that coincides exactly with the hypersurface integral. However, the extrapolative approach is able to achieve good accuracy on hypersurfaces with corners, while the original approach does not perform well on any hypersurfaces with singularities. Unlike the original approach, the extrapolative one looks at a family of functionals in  $\eta$ , where  $\eta$  is the distance from a shifted level set and the hypersurface. In that case, if the singularity is a corner, the family of functionals will be a polynomial in  $\eta$  and thus, the accuracy will depend on the number of vanishing moments of the kernel. This approach is therefore capable of achieving high accuracy for computations of integrals over piecewise smooth hypersurfaces. For cusps, the family of functionals is not polynomial in  $\eta$  but a series with fractional powers in  $\eta$ . In that case, our analysis suggests that it is necessary to construct a different class of kernels with “fractional vanishing moments” in order to achieve high accuracy. Nevertheless, this extrapolative approach provides a stepping stone towards computing over hypersurfaces with singularities. In addition, we have shown a numerical simulation that suggests the potential of this technique for integrating functions with integrable singularities.

## 6 Conclusion

We described an extrapolative approach for integrating over hypersurfaces in the level set framework. This method is based on the classical integral formulation using an approximation of the Dirac delta function typically used with level sets. This analytical integral formulation is for most cases an approximation of the integral one wishes to compute. We show that for smooth interfaces, if the kernel approximating the Dirac delta function has enough vanishing moments, the integral formulation is actually equal to the hypersurface integral. In addition, unlike previous numerical integration schemes for level sets, we demonstrate that this method is capable of computing a line or surface integral with very high accuracy in the case where the hypersurface is only piecewise smooth (e.g. with corners). Finally, with an appropriate choice of kernel approximating the Dirac delta function, we can also compute integrals where the integrand has an integrable singularity. In particular, this work lays the foundation of a numerical scheme for computing general improper integrals.

## Acknowledgement

Kublik is supported by a University of Dayton Research Council Seed Grant. Tsai is supported partially by a National Science Foundation Grant DMS-1318975 and an ARO Grant No. W911NF-12-1-0519. Tsai also thanks National Center for Theoretical Sciences, Taiwan, for hosting his stay at the center where part of the research for this paper was conducted.

## References

- [1] C. Chen, C. Kublik, and R. Tsai. An implicit boundary integral method for interfaces evolving by Mullins-Sekerka dynamics. *Submitted*.
- [2] C. Chen and R. Tsai. Implicit boundary integral methods for the Helmholtz equation in exterior domains. *UCLA CAM Report 16-38*.
- [3] L.-T. Cheng and Y.-H. Tsai. Redistancing by flow time dependent Eikonal equation. *J. Comput. Phys.*, 227(2):4002–4017, 2008.
- [4] J. Dolbow and I. Harari. An efficient finite element method for embedded interface problems. *J. Numer. Methods Eng.*, 78:229–252, 2009.
- [5] B. Engquist, A.-K. Tornberg, and R. Tsai. Discretization of dirac delta functions in level set methods. *J. Comput. Phys.*, 207(1):28–51, 2005.
- [6] C. Kublik, N. M. Tanushev, and R. Tsai. An Implicit Interface Boundary Integral Method for Poisson’s Equation on Arbitrary Domains. *J. Comput. Phys.*, 247:269–311, 2013.
- [7] C. Kublik and R. Tsai. Integration over curves and surfaces defined by the closest point mapping. *Research in the Mathematical Sciences*, 3:1–17, 2016.
- [8] W. Lorensen and H. Cline. Marching cubes: a high resolution 3d surface construction algorithm. *Computer Graphics*, 21, 1987.

- [9] E. Maître and F. Santosa. Level set methods for optimization problems involving geometry and constraints ii. optimization over a fixed surface. *Journal of Comput. Phys.*, 227:9596–9611, 2008.
- [10] S. Osher and R. Fedkiw. *Level Set Methods and Dynamics Implicit Surfaces*. Springer-Verlag, 2002.
- [11] S. Osher and F. Santosa. Level set methods for optimization problems involving geometry and constraints i. frequencies of a two-density inhomogeneous drum. *Journal of Comput. Phys.*, 171:272–288, 2001.
- [12] S. Osher and J. A. Sethian. Fronts propagating with curvature dependent speed: Algorithms based on hamilton-jacobi formulations. *J. Comp. Phys.*, 79:12–49, 1988.
- [13] G. Russo and P. Smereka. A remark on computing distance functions. *J. Comput. Phys.*, 163:51–67, 2000.
- [14] P. Schwartz, D. Adalsteinsson, P. Collela, A. P. Arkin, and M. Onsum. Numerical computation of diffusion on a surface. *Proc. Natl. Acad. Sci. USA*, 102:11151–11156, 2005.
- [15] J. Sethian. A fast marching level set method for monotonically advancing fronts. *Proceedings of the National Academy of Sciences*, 93(4):1591–1595, 1996.
- [16] J. A. Sethian. *Level Set Methods and Fast Marching Methods*. Cambridge University Press, 1999.
- [17] P. Smereka. The numerical approximation of a delta function with application to level set methods. *J. Comput. Phys.*, 211(1):77–90, 2006.
- [18] J. D. Towers. Two methods for discretizing a delta function supported on a level set. *J. Comput. Phys.*, 220(2):915–931, 2007.
- [19] Y.-H. Tsai, L.T. Cheng, S. Osher, and H.-K. Zhao. Fast sweeping methods for a class of hamilton-jacobi equations. *SIAM Journal on Numerical Analysis*, 41(2):673–694, 2003.
- [20] J. Tsitsiklis. Efficient algorithms for globally optimal trajectories. *IEEE Transactions on Automatic Control*, 40:1528–1538, 1995.
- [21] S. Zahedi and A.-K. Tornberg. Delta function approximations in level set methods by distance function extension. *J. Comput. Phys.*, 229(6):2199–2219, 2010.